



THE UNIVERSITY *of* EDINBURGH

## Edinburgh Research Explorer

# Benchmarking to the Gold Standard: Hyaluronan-oxime Hydrogels Recapitulate Xenograft Models with In Vitro Breast Cancer Spheroid Culture

### Citation for published version:

Baker, AEG, Bahlmann, LC, Tam, RY, Liu, JC, Ganesh, AN, Mitrousis, N, Marcellus, R, Spears, M, Bartlett, J, Cescon, D, Bader, GD & Shoichet, MS 2019, 'Benchmarking to the Gold Standard: Hyaluronan-oxime Hydrogels Recapitulate Xenograft Models with In Vitro Breast Cancer Spheroid Culture', *Advanced Materials*. <https://doi.org/10.1002/adma.201901166>

### Digital Object Identifier (DOI):

[10.1002/adma.201901166](https://doi.org/10.1002/adma.201901166)

### Link:

[Link to publication record in Edinburgh Research Explorer](#)

### Document Version:

Peer reviewed version

### Published In:

Advanced Materials

### General rights

Copyright for the publications made accessible via the Edinburgh Research Explorer is retained by the author(s) and / or other copyright owners and it is a condition of accessing these publications that users recognise and abide by the legal requirements associated with these rights.

### Take down policy

The University of Edinburgh has made every reasonable effort to ensure that Edinburgh Research Explorer content complies with UK legislation. If you believe that the public display of this file breaches copyright please contact [openaccess@ed.ac.uk](mailto:openaccess@ed.ac.uk) providing details, and we will remove access to the work immediately and investigate your claim.



# Advanced Materials

## Benchmarking to the Gold Standard: Hyaluronan-oxime Hydrogels Recapitulate Xenograft Models with In Vitro Breast Cancer Spheroid Culture --Manuscript Draft--

<b>Manuscript Number:</b>	adma.201901166R1
<b>Full Title:</b>	Benchmarking to the Gold Standard: Hyaluronan-oxime Hydrogels Recapitulate Xenograft Models with In Vitro Breast Cancer Spheroid Culture
<b>Article Type:</b>	Communication
<b>Section/Category:</b>	
<b>Keywords:</b>	hyaluronic acid; hydrogels; drug screening; breast cancer; 3D cell culture
<b>Corresponding Author:</b>	Molly S. Shoichet, Ph.D. University of Toronto Toronto, CANADA
<b>Additional Information:</b>	
<b>Question</b>	<b>Response</b>
Please submit a plain text version of your cover letter here.	<p>Molly Shoichet, PhD, FRS, O.C., O.Ont. University Professor Molly.shoichet@utoronto.ca 416-978-1460</p> <p>May 10, 2019</p> <p>Floriano Cuccureddu, Editor Advanced Materials</p> <p>Re: Communication, No. adma.201901166 "Benchmarking to the Gold Standard: Hyaluronan-oxime Hydrogels Recapitulate Xenograft Models with In Vitro Breast Cancer Spheroid Culture"</p> <p>Dear Dr. Cuccureddu:</p> <p>We want to thank you and the reviewers for thoughtful consideration of our manuscript. We must admit that we were surprised by your decision to reject our paper based on the reviews, which required only clarification of the text and no new experiments. Moreover, the Reviewers were generally positive, highlighting the importance of validating novel hydrogels for 3D culture – something that we rarely see in the published literature. This burgeoning field is now exploding to include organoid culture, yet the same poor choice of Matrigel is being pursued therein. We have a unique and innovative material that enables critical questions in biology to be answered.</p> <p>While Reviewer #1 suggested that our paper be considered in a sister journal, Reviewer #2 indicated that our paper should be published in this journal; both Reviewers 1 and 2 rated the originality of our submission with an acceptable level of new results; Reviewer #1 rated the scientific and technical content as fully consistent and accurate while Reviewer #2 highlighted only minor inconsistencies; both Reviewers 1 and 2 found the length concise and correct.</p> <p>We have prepared a detailed response and revised our manuscript accordingly.</p>

	<p>We respectfully request that you re-consider your decision and send our revised paper out for re-review. We are confident that this revised paper is clearer and stronger and that the novel chemistry described makes Advanced Materials the most appropriate journal for its publication.</p> <p>Sincerely,</p> <p>Molly Shoichet, PhD, FRS, O.C., O.Ont. University Professor Tier 1 Canada Research Chair, Tissue Engineering</p>
Do you or any of your co-authors have a conflict of interest to declare?	No. The authors declare no conflict of interest.
<b>Corresponding Author Secondary Information:</b>	
<b>Corresponding Author's Institution:</b>	University of Toronto
<b>Corresponding Author's Secondary Institution:</b>	
<b>First Author:</b>	Alexander E. G. Baker
<b>First Author Secondary Information:</b>	
<b>Order of Authors:</b>	<p>Alexander E. G. Baker</p> <p>Laura C. Bahlmann</p> <p>Roger Y. Tam</p> <p>Jeffrey C. Liu</p> <p>Ahil N. Ganesh</p> <p>Nikolaos Mitrousis</p> <p>Richard Marcellus</p> <p>Melanie Spears</p> <p>John M. S. Bartlett</p> <p>David W. Cescon</p> <p>Gary D. Bader</p> <p>Molly S. Shoichet, Ph.D.</p>
<b>Order of Authors Secondary Information:</b>	
<b>Abstract:</b>	<p>Many 3D in vitro models induce breast cancer spheroid formation; however, this alone does not recapitulate the complex in vivo phenotype. To effectively screen therapeutics, we urgently need to validate in vitro cancer spheroid models against the gold standard of xenografts. We designed a new oxime-crosslinked hyaluronan (HA) hydrogel, manipulating gelation rate and mechanical properties to grow breast cancer spheroids in 3D. Our HA-oxime breast cancer model maintains the gene expression profile most similar to that of tumour xenografts based on a pan-cancer gene expression profile (comprising 730 genes) of 3 different human breast cancer subtypes compared to Matrigel or conventional 2D culture. Differences in gene expression between breast cancer cultures in HA-oxime versus Matrigel or 2D were confirmed for 12 canonical pathways by gene set variation analysis. Importantly, drug response was dependent on the culture method. Breast cancer cells responded better to the Rac inhibitor (EHT-1864) and the PI3K inhibitor (AZD6482) when cultured in HA-oxime versus Matrigel. This study demonstrates, for the first time, the superiority of an HA-based hydrogel as a platform for in vitro breast cancer culture of both primary, patient-derived cells and cell lines, and provides a hydrogel culture model that closely matches</p>

that in vivo.

# Benchmarking to the Gold Standard: Hyaluronan-oxime Hydrogels Recapitulate Xenograft Models with *In Vitro* Breast Cancer Spheroid Culture

*Alexander E. G. Baker, Laura C. Bahlmann, Roger Y. Tam, Jeffrey C. Liu, Ahil N. Ganesh, Nikolaos Mitrousis, Richard Marcellus, Melanie Spears, John M. S. Bartlett, David W. Cescon, Gary D. Bader, Molly S. Shoichet\**

Dr. A. E. G. Baker, L. C. Bahlmann, Dr. R. Y. Tam, Dr. J. C. Liu, Dr. A. N. Ganesh, Dr. N. Mitrousis, Prof. G. D. Bader, Prof. M. S. Shoichet  
The Donnelly Centre, University of Toronto, Toronto, 160 College St, Ontario, M5S 3E1, Canada

Dr. A. E. G. Baker, Dr. R. Y. Tam, Dr. A. N. Ganesh, Prof. M. S. Shoichet  
Department of Chemical Engineering and Applied Chemistry, University of Toronto, 200 College Street, Toronto, Ontario, M5S 3E5, Canada

Dr. A. E. G. Baker, L. C. Bahlmann, Dr. R. Y. Tam, Dr. J. C. Liu, Dr. A. N. Ganesh, Dr. N. Mitrousis, Prof. M. S. Shoichet  
Institute of Biomaterials and Biomedical Engineering, 164 College Street, Toronto, Ontario, M5S 3G9, Canada

Dr. R. Marcellus, Dr. M. Spears, Dr. J. M. S. Bartlett  
Ontario Institute for Cancer Research, MaRS Centre, 661 University Avenue, Toronto, Ontario, M5G 0A3, Canada

Dr. M. Spears  
Department of Laboratory Medicine and Pathology, University of Toronto, 1 King's College Circle, Toronto, Ontario, M5S 1A8, Canada

Dr. D. W. Cescon  
Princess Margaret Cancer Centre, University Health Network, 610 University Ave, Toronto, Ontario, M5G 2C1, Canada

Prof. M. S. Shoichet  
Department of Chemistry, University of Toronto, 80 St. George Street, Toronto, Ontario, M5S 3H6, Canada

\* To whom all correspondence should be addressed:

e-mail: molly.shoichet@utoronto.ca

## Keywords

Hyaluronic Acid, Hydrogels, Drug Screening, Breast Cancer, 3D Cell Culture

## Abstract

Many 3D *in vitro* models induce breast cancer spheroid formation; however, this alone does not recapitulate the complex *in vivo* phenotype. To effectively screen therapeutics, we urgently need

1  
2  
3  
4 to validate *in vitro* cancer spheroid models against the gold standard of xenografts. We designed a  
5  
6 new oxime-crosslinked hyaluronan (HA) hydrogel, manipulating gelation rate and mechanical  
7  
8 properties to grow breast cancer spheroids in 3D. Our HA-oxime breast cancer model maintains  
9  
10 the gene expression profile most similar to that of tumour xenografts based on a pan-cancer gene  
11  
12 expression profile (comprising 730 genes) of 3 different human breast cancer subtypes compared  
13  
14 to Matrigel or conventional 2D culture. Differences in gene expression between breast cancer  
15  
16 cultures in HA-oxime versus Matrigel or 2D were confirmed for 12 canonical pathways by gene  
17  
18 set variation analysis. Importantly, drug response was dependent on the culture method. Breast  
19  
20 cancer cells responded better to the Rac inhibitor (EHT-1864) and the PI3K inhibitor (AZD6482)  
21  
22 when cultured in HA-oxime versus Matrigel. This study demonstrates, for the first time, the  
23  
24 superiority of an HA-based hydrogel as a platform for *in vitro* breast cancer culture of both  
25  
26 primary, patient-derived cells and cell lines, and provides a hydrogel culture model that closely  
27  
28 matches that *in vivo*.  
29  
30  
31  
32  
33  
34  
35  
36

## 37 **Main**

38  
39 Despite improvements in initial target identification using computational approaches,<sup>[1]</sup>  
40  
41 and several proposed hydrogels to culture cells for the *in vitro* stage of drug discovery,<sup>[2]</sup> two-  
42  
43 dimensional (2D) culture on tissue culture poly(styrene) (TCPS) continues to be used to screen  
44  
45 cancer therapeutics. 2D culture does not represent the *in vivo* microenvironment either  
46  
47 mechanically or biochemically, thereby leading to false positive (and likely false negative) drug  
48  
49 hits.<sup>[3]</sup> *In vivo* xenograft tumour models recapitulate human disease more faithfully, but are costly,  
50  
51 time-consuming and complicated by the use of immunocompromised mice.<sup>[4]</sup> The inaccurate but  
52  
53 rapid and simple method of testing drugs in 2D coupled with the complexity of xenograft models,  
54  
55 has motivated the development of more representative three-dimensional (3D) culture platforms.  
56  
57  
58  
59  
60  
61  
62  
63  
64  
65

1  
2  
3  
4 A suitable 3D culture system must be sufficiently stable for drug screening and benchmarked  
5  
6 against gold standard *in vivo* xenograft tumour models.<sup>[5]</sup> The limited availability of such 3D  
7  
8 models results in the continued reliance on 2D culture, even with the recognition that 2D culture  
9  
10 does not accurately predict *in vivo* outcomes.  
11  
12  
13

14  
15 Unlike 2D culture, where breast epithelial cancer cells form a monolayer, 3D models of  
16  
17 cancer recapitulate many disease characteristics such as formation of cancer spheroids with tight  
18  
19 junctions, and inclusion of key biochemical and mechanical cues of the native extracellular matrix  
20  
21 (ECM).<sup>[6]</sup> Typically, cancer spheroids are formed by growing epithelial cancer cells in 3D using  
22  
23 non-adherent conditions. This method is rapid and provides remarkable control of the spheroid  
24  
25 size;<sup>[7]</sup> yet, unsurprisingly, the gene expression profiles of these cancer spheroids (CS) formed by  
26  
27 aggregation resemble cells cultured in 2D more closely than those of xenograft tumours.<sup>[8]</sup>  
28  
29 Therefore, spheroid formation alone does not recapitulate the *in vivo* microenvironment.<sup>[9]</sup> Non-  
30  
31 adherent conditions lack critical ECM components, which both affect cell function through  
32  
33 integrin-mediated signaling pathways, such as  $\beta 1$ , and influence drug effectiveness.<sup>[10]</sup>  
34  
35  
36  
37  
38  
39

40 Laminin-rich extracellular matrices, such as Matrigel®, which is derived from the  
41  
42 Engelbreth-Holm-Swarm murine sarcoma, are favored for 3D cell culture as they contain some  
43  
44 physiologically relevant ECM proteins that mimic the breast tumour microenvironment.<sup>[11]</sup>  
45  
46 However, Matrigel is ill-defined,<sup>[12]</sup> and its composition, physicochemical and biomechanical  
47  
48 properties have limited tunability.<sup>[13]</sup> Moreover, Matrigel does not include key matrix components  
49  
50 found in the breast cancer microenvironment such as hyaluronan (HA), which is produced by  
51  
52 tumour and stromal cells and is linked to disease progression.<sup>[14]</sup> The diversity of cell-surface  
53  
54 integrin expression and tumour microenvironment properties across breast cancer subtypes require  
55  
56 a model that is tunable to meet these complexities.<sup>[15]</sup>  
57  
58  
59  
60  
61  
62  
63  
64  
65

The majority of chemically crosslinked hydrogels utilize chemistries that have rapid reaction kinetics,<sup>[16]</sup> such as the thiol-Michael addition ligation,<sup>[17]</sup> and limit uniform cell encapsulation, making reproducible *in vitro* cell culture challenging. Moreover, many scaffold components need to be stored under inert gas due to air-sensitive functional groups, such as thiols, and/or require external stimuli to promote crosslinking, which complicates scale up.<sup>[18, 19]</sup> To achieve a more controlled system for cell encapsulation, we combined fast-reacting HA-aldehyde and slow-reacting HA-ketone with poly(ethylene glycol) (PEG)-oxyamine to create defined 3D hydrogels via oxime click chemistry. Oxime ligation is hydrolytically stable, thereby allowing long-term encapsulation of breast cancer cells – a key advance over current strategies that are inherently limited by reversible reactions of hydrazone or Diels-Alder chemistries for crosslinking.<sup>[20, 21]</sup> In addition, the oxime chemistry is insensitive to oxidation, facile to use and enables controlled gelation rates, which is typically not possible with other click chemistry reactions.<sup>[18]</sup> We used these newly synthesized oxime-crosslinked HA hydrogels to benchmark the gene expression of breast cancer cells against tumour xenografts grown in mice and evaluate drug response in comparison with conventional culture in Matrigel and 2D TCPS (Fig. 1a).

## Synthesis of HA-oxime Hydrogels

We synthesized HA-oxime gels with HA-ketone (HAK), HA-aldehyde (HAA) and PEG-oxyamine, each component of which first needed to be synthesized. HAK was synthesized, for the first time, in a two-step reaction: (1) amide coupling of 3-(2-methyl-1,3-dioxolan-2-yl)propan-1-amine with 4-(4,6-dimethoxy-1,3,5-triazin-2-yl)-4-methylmorpholinium chloride (DMTMM) as an activator and (2) acid-catalyzed ketone deprotection (Fig. 1b). We found the substitution of ketone to be tunable between  $28 \pm 3\%$  and  $55 \pm 2\%$  by increasing the equivalents of DMTMM from 1.0 to 2.5, respectively (Fig. S1). We chose to use HAK with approximately 40% ketone



substitution to produce hydrogels because it was water soluble and easy to handle. Similarly, we synthesized aldehyde-modified HA (HAA) in two steps: (1) amidation of carboxylic acid groups on HA with DMTMM/aminoacetaldehyde dimethyl acetal, and (2) deprotection of the resulting HA-acetal with aqueous acid (Fig. 1c, Fig S2). The PEG-substituted oxyamine crosslinker was prepared from either 4-arm PEG-tetramine or 2-arm PEG-bisamine and (boc-aminoxy)acetic acid with carbodiimide coupling followed by acid-catalyzed deprotection to yield PEGOA<sub>4</sub> and PEGOA<sub>2</sub>, respectively (Fig. S2).

We combined HAK and HAA with PEGOA<sub>4</sub> and laminin (a common extracellular matrix protein) to produce crosslinked hydrogels with tunable biochemical properties to grow breast cancer spheroids (Fig. 1d). To show that both HAK and HAA biopolymers were crosslinked with PEG-oxyamine, we compared the stability of hydrogels comprised of equal weight percent of either HAK/HAA or unmodified-HA/HAA crosslinked with PEG-oxyamine: HAK/HAA hydrogels remained stable over at least 28 days (with less than 5% decrease in mass) whereas gels formed from HA/HAA slowly dissociated, losing  $50 \pm 2\%$  of their mass between day 1 and 28, reflecting the dissolution of uncrosslinked HA (Fig. S3). Gels crosslinked with four-armed PEGOA<sub>4</sub> swelled significantly less than those crosslinked with bifunctional PEGOA<sub>2</sub> (Fig. S3). Although both remained intact over four weeks, we used PEGOA<sub>4</sub> in all subsequent experiments because the increased swelling of PEGOA<sub>2</sub> crosslinked gels would alter hydrogel mechanical properties and hence cell phenotype.<sup>[22]</sup>

### **Tunable Gelation of HA-oxime Hydrogels Influences 3D Cell Distribution**

To achieve uniform 3D cell distribution, hydrogels must form rapidly enough to avoid cell aggregation due to gravity during gelation, but slow enough for practical use. HAA only crosslinked hydrogels (0:1 HAK:HAA) formed too quickly for cell encapsulation, requiring cells

1  
2  
3  
4 to be cultured on top of those gels versus within.<sup>[21]</sup> In contrast, hydrogels synthesized with only  
5  
6 HAK (1:0, HAK:HAA) and PEGOA<sub>4</sub> formed too slowly, with gelation at  $87 \pm 11$  min.  
7  
8 Consequently, when single breast cancer cells were encapsulated in HAK-only HA-oxime gels,  
9  
10 cells accumulated in the bottom of the well, due to the slow crosslinking reaction between ketones  
11  
12 and oxyamines (Fig. 1e). We used rheology to characterize the gelation rate of HA-oxime  
13  
14 hydrogels with varying HAK:HAA mass ratios (Fig. S4). The gelation rate increased significantly  
15  
16 with an increasing amount of HAA (Fig. 1f). HA-oxime hydrogels produced with HAK:HAA mass  
17  
18 ratios of either 7:1 or 3:1, at a constant oxyamine to ketone/aldehyde mole ratio of 0.60, resulted  
19  
20 in mean gelation times of 35 and 25 min, respectively. At higher weight percentages of the faster  
21  
22 gelling HAA (HAK:HAA of 1:1), the resulting crosslinked gel formed too rapidly for  
23  
24 quantification by rheology. We used HAK:HAA of 3:1 in subsequent assays and found a uniform  
25  
26 distribution of viable cells (Fig. S5). This uniform distribution was maintained for a longer time  
27  
28 when cells were grown in HA-oxime hydrogels versus those in Matrigel or a commercially  
29  
30 available HA-based hydrogel, HyStem-C (HA-thiol/gelatin-thiol crosslinked with PEG diacrylate)  
31  
32 (Fig. S5c).

### 33 34 35 36 37 38 39 40 41 42 **Composition-controlled Mechanical Properties and Enzyme-specific Degradation of HA-** 43 44 **oxime Hydrogels**

45  
46 We were interested in understanding the mechanical tunability of HA-oxime hydrogels in  
47  
48 relation to Matrigel, the current standard for 3D cell and organoid culture. Matrigel compositions,  
49  
50 purchased with protein concentrations of 8.50 and 18.43 mg·mL<sup>-1</sup>, had compressive moduli of 0.9  
51  
52  $\pm 0.7$  kPa and  $1.6 \pm 0.4$  kPa, respectively, which were not significantly different from each other  
53  
54 (Fig. 1g). These formulations are typically used for *in vitro* culture and underscore the limited  
55  
56 mechanical tunability offered by Matrigel.<sup>[23]</sup> In contrast, the stiffness of HA-oxime hydrogels  
57  
58  
59  
60  
61  
62  
63  
64  
65

varied with the ratio of HAK to HAA. HA-oxime hydrogels are highly tunable over 2 orders of magnitude, between 0.3 and 15 kPa, by either varying the crosslinking density or the weight percent of HA (Fig. S6). This range covers the stiffness reported for mouse mammary tumours (~1.5-4.0 kPa), and human breast cancer tissue (~5-16 kPa), as measured by compression and atomic force microscopy, respectively.<sup>[24, 25]</sup>

HAK-only (1.35 wt%) hydrogels were significantly stiffer ( $15 \pm 1$  kPa) than HAA-only (1.35 wt%) hydrogels ( $5.5 \pm 0.4$  kPa) at a constant mole ratio (0.80) of oxyamine to ketone/aldehyde (Fig. S6). We attributed this difference in modulus of HAK-oxime and HAA-oxime hydrogels to the difference in molar mass. While we started with the same molar mass of HA, synthesis of HAK resulted in a molar mass of  $311 \text{ kg}\cdot\text{mol}^{-1}$  whereas that of HAA resulted in a molar mass of  $122 \text{ kg}\cdot\text{mol}^{-1}$  as measured by gel permeation chromatography. Importantly, there was no change in oxyamine to oxime conversion with all HAK and HAA formulations, as quantified by  $^1\text{H}$  NMR spectroscopy (Fig. S7), further indicating that the molar mass difference accounted for the difference in compressive modulus. The stiffness of gel formulations with 3:1 and 1:1 HAK:HAA weight ratios were not statistically different from Matrigel, so we used 3:1 ratio for future experiments as it was easier to handle. We found that these HA-oxime gels were stable for 28 days when swollen in PBS or when treated with collagenase and degraded only in the presence of hyaluronidase, highlighting the enzyme-specific degradability (Fig. 1h). Importantly, breast cancer cells are known to produce hyaluronidase, which allows dynamic, cell-based spatiotemporal remodeling of the HA-oxime hydrogels during cell growth.<sup>[26]</sup>

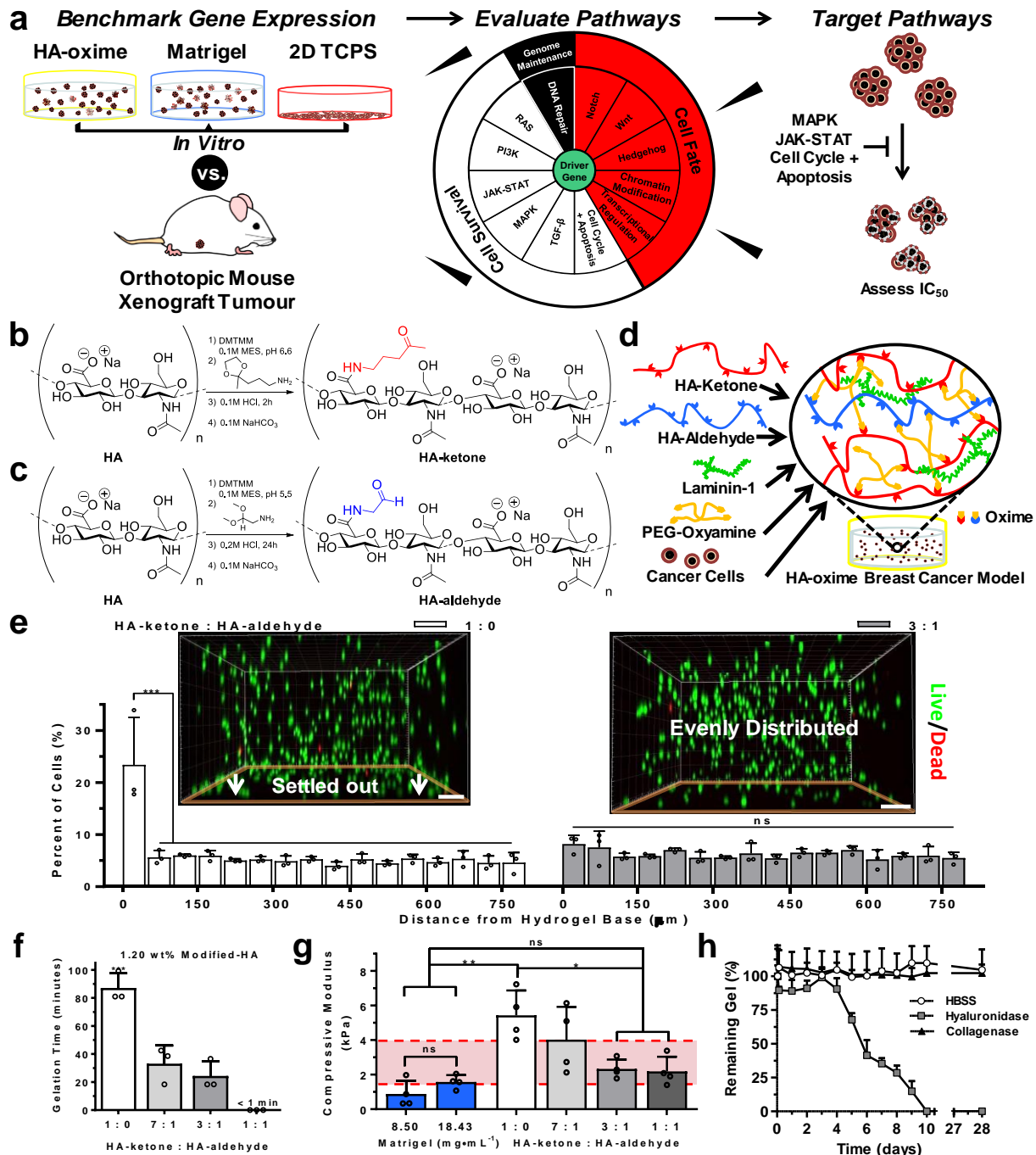


**Figure 1.** Synthesis and characterization of the HA-oxime hydrogel to model breast cancer in vitro.

(a) The overall goal was to benchmark the gene expression profile of cells cultured in vitro in our novel HA-oxime hydrogels relative to conventional culture in either Matrigel or 2D tissue culture polystyrene (TCPS) to those cells grown in vivo. This methodology allows us to identify pathways

that can then be targeted in drug screening assays. (b) Synthesis of HA-ketone using DMTMM coupling to HA with 3-(2-methyl-1,3-dioxolan-2-yl)propan-1-amine followed by acid-catalyzed deprotection, and neutralization. (c) Synthesis of HA-aldehyde using DMTMM coupling with aminoacetaldehyde dimethyl acetal followed by acid-catalyzed deprotection, and neutralization. (d) HA-oxime crosslinked hydrogels comprised of HA-ketone (HAK, red), HA-aldehyde (HAA, blue), and poly(ethylene glycol)-tetraoxyamine (PEGOA<sub>4</sub>, orange) and formed in the presence of laminin (green) and breast cancer cells (tan), which resulted in uniformly distributed cells. (e) Distribution of encapsulated MDA-MB-468 cells after 24 h in HA-oxime hydrogels: in HAK crosslinked gels, cells aggregate at the bottom of the well due to the slow gelation whereas in HAK:HAA (3:1 mass ratio), cells are evenly distributed. Cells were stained for viability with calcein AM (live, green) and ethidium homodimer-1 (dead, red); scale bar represents 200  $\mu\text{m}$  (n = 3 independent experiments; mean + s.d. plotted, \*\*\*p<0.001, one-way ANOVA, Tukey's post-hoc test). (f) Gelation time of HA-oxime hydrogels crosslinked with PEGO<sub>4</sub> (n = 3, mean + s.d., \*\*\*p<0.001, one-way ANOVA, Tukey's post-hoc test). (g) Compressive modulus of HA-oxime hydrogels compared to growth factor reduced Matrigel (n = 4, mean + s.d. plotted, \*p<0.05; \*\*p<0.01, one-way ANOVA, Tukey's post-hoc test). The red shaded area represents the range in stiffness of mouse tumours reported in the literature.<sup>[24]</sup> (h) HA-oxime hydrogel prepared from 3:1 HA-ketone (0.90 wt%) and HA-aldehyde (0.30 wt%) crosslinked with PEGO<sub>4</sub> (1.04 wt%) was stable over 28 days at 37 °C in Hank's balanced salt solution (HBSS) and in the presence of collagenase, but degraded in the presence of hyaluronidase. The percent of remaining hydrogel was determined from the mass measurements (n = 3, mean + s.d. plotted).

### **Biochemically-tuned Laminin-containing HA-oxime Hydrogels Interact with Cells**

To mimic the heterogeneity of the extracellular matrix in breast cancer and enhance cell interaction with the HA-oxime hydrogels,<sup>[27]</sup> we mixed laminin-1 (Ln) with the polymers prior to gelation and found that it was retained in the gels obviating the need for covalent immobilization: Ln incorporated at either 75 or 250  $\mu\text{g}\cdot\text{mL}^{-1}$  was completely retained in hydrogels after 7 days, with no soluble Ln detected in the PBS supernatant (Fig. 2a). Given the large size of Ln (850 kDa), it was likely physically entrapped or entangled within the HA-oxime polymer chains, but may have also be retained by either (or both) electrostatic interactions between positively charged Ln and negatively charged hyaluronan-carboxylate groups<sup>[28]</sup> or reversible Schiff-base formation between basic lysine groups on laminin and HA-ketone/aldehyde groups.<sup>[29]</sup> The interactions between laminin and HA-oxime hydrogels did not alter the compressive modulus compared to HA-oxime only hydrogels thereby enabling the role of ECM proteins to be studied separately from mechanical properties (Figs. S8a).

To investigate cell-Ln interactions, we compared cell adhesion to HA-oxime gels with or without Ln and found more than 2-times more T47D luminal A breast cancer cells adhered to the surface of hydrogels containing 75  $\mu\text{g}\cdot\text{mL}^{-1}$  Ln, similar to Matrigel versus controls without Ln (Fig. 2b). With or without Ln, breast cancer cells encapsulated in HA-oxime hydrogels were equally viable and evenly distributed, and the size and number of spheroids were similar (Fig. S8b-i). Cells within the spheroids interacted with each other, as demonstrated by E-cadherin expression, a marker of tight junctions (Fig. 2c-d). Cells also interacted with the HA-oxime hydrogel through CD44, a hyaluronan receptor, and expressed  $\beta 1$ -integrin, a Ln receptor (Fig. 2e-h). CD44 is essential to the growth of breast cancer cells and  $\beta 1$ -integrin is involved in the PI3K pathway, which is upregulated in breast cancer and constitutes a drug target.<sup>[30]</sup> We observed some evidence of HIF-1 $\alpha$  expression, a marker for either reactive oxygen species or hypoxia typically observed

in breast cancer tumours (Fig. 2i-j). The HIF-1 $\alpha$  expression observed at the periphery of the spheroids has been observed in other cancer spheroids and likely represents reactive oxygen species versus hypoxia at the core because oxygen can diffuse through the  $\sim 70$   $\mu\text{m}$  diameter spheroids (Fig. S9).<sup>[31]</sup> Given the relevance of hyaluronan in breast cancer<sup>[32]</sup> and the interaction of cells with the HA-oxime hydrogels, we wondered whether culture in HA-oxime with or without laminin would impact the gene expression levels compared to those in Matrigel and conventional 2D TCPS.

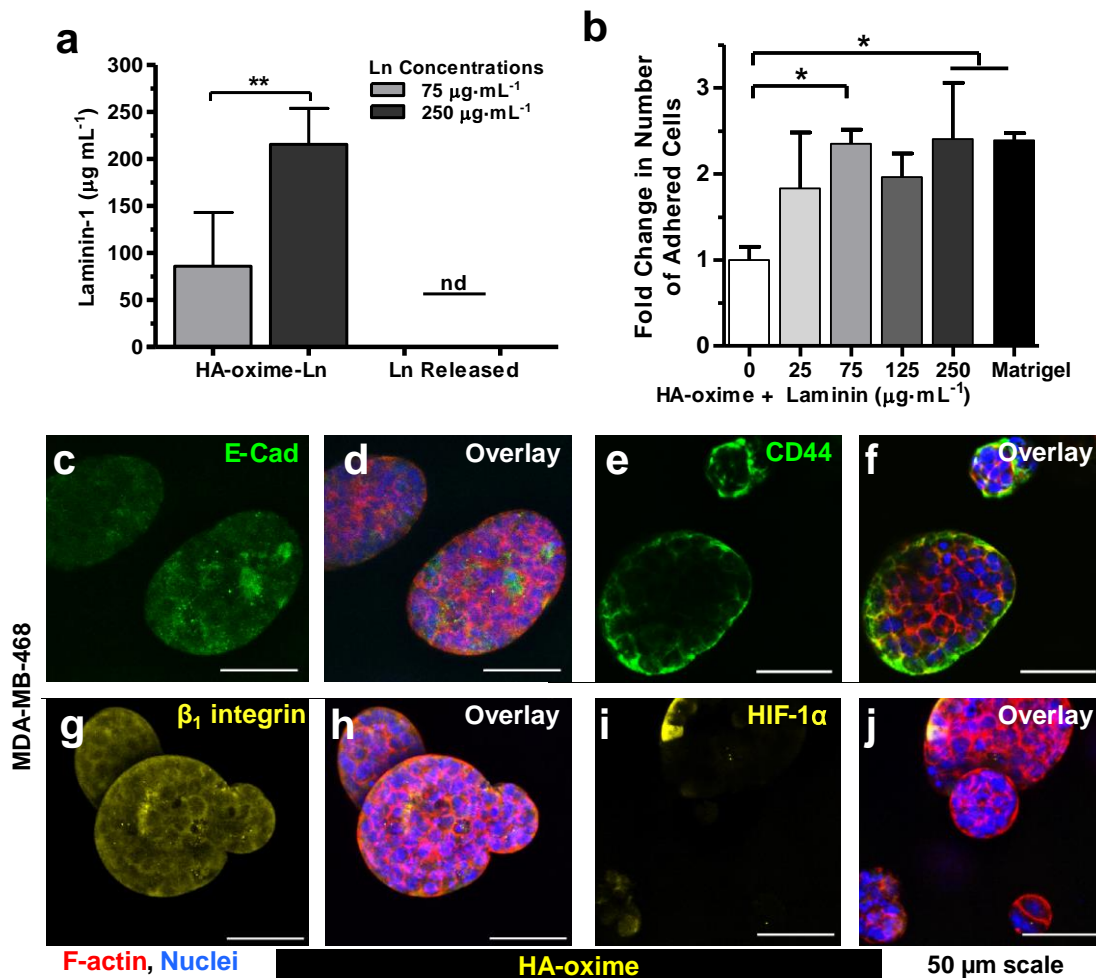


**Figure 2.** Impact of laminin in HA-oxime hydrogels. (a) The amount of Ln retained in HA-oxime hydrogels crosslinked with PEGOA<sub>4</sub> quantified by ELISA after 7 days, Ln was not detected (nd) from supernatant 24 h after adding PBS to HA-oxime-Ln hydrogels (n = 3 independent samples;

mean + standard deviation plotted, no significant differences (ns), \*\* $p < 0.01$ , one-way ANOVA, Tukey's post-hoc test). (b) Fold change in the number of breast cancer cells on HA-oxime gels crosslinked with PEGOA<sub>4</sub> containing Ln versus those on Matrigel (n = 3 independent studies; mean + standard deviation plotted, \* $p < 0.05$ ; one-way ANOVA, Tukey's post-hoc test). (c-j) Representative immunocytochemistry images of MDA-MB-468 cells encapsulated in HA-oxime hydrogels after 21 days stained for nuclei (with Hoechst, blue) and actin (with phalloidin which binds to F-actin, red) (c, d) E-cadherin, (e, f) CD44, (g, h)  $\beta_1$  integrin and (i, j) HIF-1 $\alpha$ .

### **HA-oxime Hydrogels Enable Spheroid Formation of 5 Different Breast Cancer Cell Lines and Patient-derived Primary Breast Cancer Cells**

When cells from 5 different breast cancer cell lines were cultured for 21 days in HA-oxime hydrogels +/- Ln they formed spheroids, which was not observed in 2D culture (Fig. S10). These cells represent 4 breast cancer subtypes with different expression profiles of estrogen receptor (ER), progesterone receptor (PR), and human epidermal growth factor receptor 2 (HER2): luminal A MCF7 and T47D (ER<sup>+</sup>, PR<sup>+</sup>, HER2<sup>-</sup>), luminal B BT474 (ER<sup>+</sup>, PR<sup>+</sup>, HER2<sup>+</sup>), HER2-overexpressing MDA-MB-231-H2N (ER<sup>-</sup>, PR<sup>-</sup>, HER2<sup>+</sup>), and triple negative MDA-MB-468 (ER<sup>-</sup>, PR<sup>-</sup>, HER2<sup>-</sup>) cells. By examining proliferation in 2D and 3D, and between different hydrogel cultures, we observed that all breast cancer cell lines exhibited similar proliferation rates in HA-oxime +/- Ln hydrogels compared to Matrigel except BT474 cells, where proliferation was increased in Matrigel (Fig. 3a). In addition, all cells formed spheroids of similar diameter ~100  $\mu$ m, suitable for oxygen and nutrient penetration<sup>[33]</sup> at 21 days in HA-oxime hydrogels and Matrigel (Fig. 3b), indicating phenotypic equivalence at minimum.

Recent efforts to develop *in vitro* cancer models that recapitulate the features of human breast cancer for preclinical testing or personalized medicine have used poorly-defined Matrigel



1  
2  
3  
4 to grow 3D tumour organoids. To test the HA-oxime hydrogel for these applications, we  
5  
6 encapsulated patient-derived primary luminal B breast cancer cells in 3D therein and observed  
7  
8 their survival and proliferation: the patient-derived cells grew as spheroids in the hydrogel but  
9  
10 proliferated as monolayers on 2D TCPS (Fig. S11). Impressively, encapsulated primary breast  
11  
12 cancer cells from a dissociated patient biopsy formed spheroids in both HA-oxime +/- Ln and  
13  
14 Matrigel after 21 days of culture (Fig. 3c-f). It is possible that over the 21 days of culture within  
15  
16 the 3D hydrogel, glucose and/or oxygen gradients will form and result in heterogeneity that more  
17  
18 closely mimics the tumour microenvironment within the xenograft versus that of 2D TCPS. These  
19  
20 results led us to perform a more extensive comparison of gene expression between the mouse  
21  
22 xenografts and *in vitro* models in order to better understand the biological differences between  
23  
24 these *in vitro* models.  
25  
26  
27  
28  
29  
30

### 31 32 **Gene Expression of 5 Distinct Breast Cancer Cell Lines Cultured *In Vitro* vs. In Vivo Growth** 33 34 **as Tumour Xenografts** 35

36  
37 In order to understand how breast cancer markers and drug-targetable pathways are  
38  
39 impacted by culture platform, we benchmarked the gene expression of 5 cell lines cultured in HA-  
40  
41 oxime +/- Ln against orthotopic mouse xenografts in NOD SCID gamma mice and compared them  
42  
43 to those in Matrigel or 2D TCPS (Fig. S12, S13). In general, the gene expression of breast cancer  
44  
45 cells cultured in either HA-oxime hydrogels +/- Ln or Matrigel were more similar to that of mouse  
46  
47 xenograft models than cells cultured on 2D TCPS (Fig. 3g). Several genes were differentially  
48  
49 expressed compared to tumour xenografts when cultured on 2D TCPS, but not when cultured in  
50  
51 HA-oxime hydrogels, including epidermal growth factor receptor (EGFR), human epidermal  
52  
53 growth factor receptor 2 (ERBB2) and phosphatidylinositol-4,5-bisphosphate 3-kinase catalytic  
54  
55 subunit alpha (PIK3CA) which are implicated in drug targetable pathways (Table S1). The  
56  
57  
58  
59  
60  
61  
62  
63  
64  
65

1  
2  
3  
4 expression of both ERBB2 and EGFR can result in changes to cell phenotype and tumourigenicity,  
5  
6 and may also influence response to therapy, including agents targeting these receptors directly.<sup>[34]</sup>  
7  
8 In addition, patients with PIK3CA-positive breast tumours have shorter disease-free survival  
9  
10 across all molecular subtypes indicating its potential as a therapeutic target.<sup>[35]</sup> Thus, these results  
11  
12 further underscore the need to use representative 3D models to study breast cancer over traditional  
13  
14 2D culture.  
15  
16

17  
18 A potential strategy for treating breast cancer beyond traditional kinase inhibitors includes  
19  
20 emerging metabolic targets such as FASN, which is responsible for lipid synthesis. Currently, the  
21  
22 FASN inhibitor TVB-2640 is being evaluated for the treatment of advanced breast cancer in a  
23  
24 clinical trial.<sup>[36]</sup> Due to observed differences in cellular fatty acid and cholesterol content between  
25  
26 2D culture and xenograft models,<sup>[37]</sup> we hypothesized that the expression of lipid metabolic genes  
27  
28 would be more similar in 3D cell culture than 2D culture relative to the xenograft tumours. The  
29  
30 expression of FASN, which is responsible for lipid synthesis, and ATP-binding cassette transporter  
31  
32 (ABCA1), which regulates intracellular phospholipid and cholesterol homeostasis, depended upon  
33  
34 both cell line and culture system. For example, luminal A MCF7 cells had similar ABCA1 and  
35  
36 FASN expression between tumour xenograft and HA-oxime hydrogel culture, but an upregulated  
37  
38 FASN expression when cultured on 2D TCPS or Matrigel (Fig. 3g). This shows that FASN  
39  
40 expression is influenced by the ECM and that gene expression levels of xenograft tumours for  
41  
42 luminal A breast cancer were recapitulated using the HA-oxime hydrogel. However, HER2-  
43  
44 overexpressing MDA-MB-231-H2N cells upregulated FASN and ABCA1 across all *in vitro*  
45  
46 models, which suggests altered lipid metabolism and secretion compared to xenograft tumours.  
47  
48 These differences in FASN expression were not observed for other breast cancer subtypes, which  
49  
50 supports breast cancer subtype-dependent lipid metabolism in 2D.<sup>[38]</sup> Considering the similar gene  
51  
52  
53  
54  
55  
56  
57  
58  
59  
60  
61  
62  
63  
64  
65

expression of breast cancer cells cultured in HA-oxime hydrogels and grown as xenograft tumours, we performed more rigorous benchmarking with a pan-cancer gene expression panel.

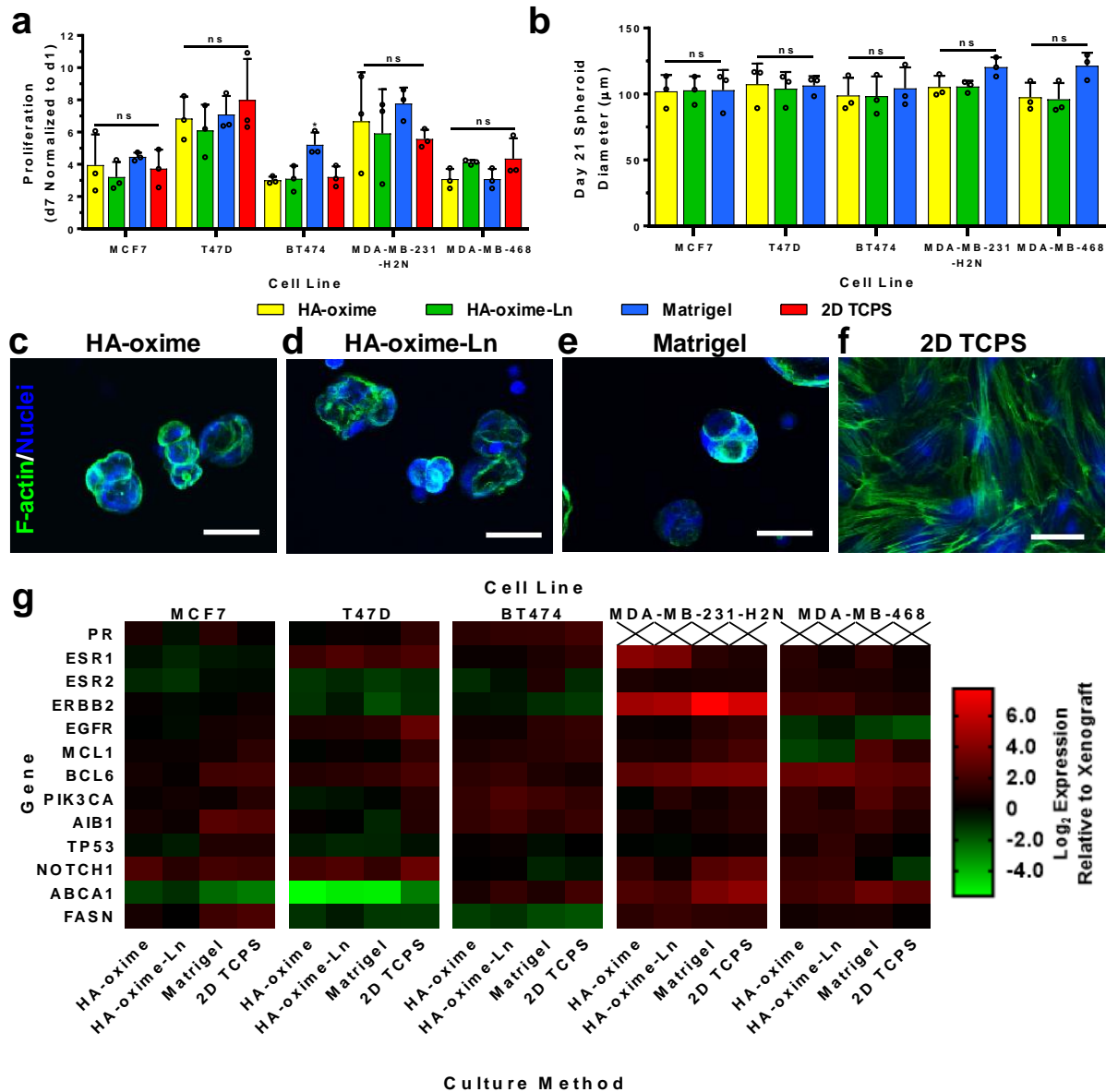


**Figure 3.** Evaluation of patient-derived and 5 different breast cancer cell lines in HA-oxime +/- Ln versus Matrigel and 2D TCPS. (a) Cell growth at day 7 relative to day 1 ( $n = 3$ ; mean + s.d. plotted,  $*p < 0.05$ , one-way ANOVA, Tukey's post-hoc test). (b) Tumour spheroid diameter after 21 days of culture for cells embedded in HA-oxime, HA-oxime-Ln or Matrigel ( $n = 3$ ; mean + s.d. plotted,  $*p < 0.05$ , one-way ANOVA, Tukey's post-hoc test). No spheroids were formed on 2D

1  
2  
3  
4 TCPS. (c-f) Representative images of primary, patient breast cancer cells after 21 days of culture  
5  
6 in (c) HA-oxime, (d) HA-oxime + Ln, (e) Matrigel or (f) 2D TCPS. Cells stained with phalloidin  
7  
8 (binds to F-actin, shown in green) and Hoechst (nuclei, shown in blue); scale bar represents 50  
9  
10  $\mu\text{m}$ . (g) Heat map gene expression of MCF7, T47D, BT474, MDA-MB-231-H2N, and MDA-MB-  
11  
12 468 cells encapsulated in HA-oxime, HA-oxime-Ln, Matrigel, or cultured on 2D TCPS after 21  
13  
14 days and compared to the respective mouse xenograft tumours. Expression reported as the Log<sub>2</sub>  
15  
16 ratio from qPCR with black indicating the greatest similarity (n = 3-5 independent studies; mean  
17  
18 plotted).

### 23 24 **Pan-Cancer Gene Expression Benchmarks *In Vitro* Breast Cancer Models**

25  
26  
27 In order to better understand the predictive powers of 3D in vitro culture of breast cancer  
28  
29 cells, we benchmarked 3 distinct cell lines, representing 3 different breast cancer subtypes, to  
30  
31 tumour xenografts: luminal B (BT474); HER2-overexpressing (MDA-MB-231-H2N); and triple  
32  
33 negative (MDA-MB-468). We cultured cells in 3D in HA-oxime, Matrigel or in 2D on TCPS and  
34  
35 compared the gene expression panel of 730 cancer-related genes. Relative to tumour xenografts,  
36  
37 we found that luminal B, BT474 cells had the fewest number of differentially expressed genes  
38  
39 when cultured in HA-oxime gels (24 downregulated and 27 upregulated of 730 genes) compared  
40  
41 to those cultured in Matrigel (63 downregulated and 135 upregulated) and on 2D TCPS (60  
42  
43 downregulated, 45 upregulated) (Fig. 4a, b, Table S2). Surprisingly, there were more differences  
44  
45 when cells were cultured in Matrigel than on 2D TCPS relative to xenografts, which both reflects  
46  
47 the unsuitability of Matrigel and demonstrates that 3D culture alone is insufficient for predictive  
48  
49 drug screening.

50  
51  
52 We analyzed 12 pathways and driver genes by gene set variation analysis and found that  
53  
54 BT474 cells cultured in Matrigel altered the expression of several pathways including JAK-STAT  
55  
56  
57  
58  
59  
60  
61  
62  
63  
64  
65

1  
2  
3  
4 and MAPK versus tumour xenografts whereas cells cultured in HA-oxime gels did not (Fig. 4c).  
5  
6 This further motivates the use of representative, benchmarked 3D *in vitro* models, such as the HA-  
7  
8 oxime hydrogel, to recapitulate gene expression and to evaluate new drug candidates against JAK-  
9  
10 STAT and MAPK.<sup>[39]</sup>  
11  
12

13  
14 Comparing the gene expression of MDA-MB-231-H2N tumours to 3D hydrogels and 2D  
15  
16 culture, we found that fewer genes were differentially expressed when cells were grown in HA-  
17  
18 oxime gels (16 downregulated, 12 upregulated) versus both Matrigel (28 downregulated, 21  
19  
20 upregulated) and 2D TCPS (33 downregulated, 29 upregulated) (Fig. 4d, e, Table S3). Altered  
21  
22 gene expression of a therapeutic target in cells used in an *in vitro* drug screen would generate  
23  
24 misleading data. Differences in the JAK-STAT pathway were identified between cells cultured in  
25  
26 HA-oxime, Matrigel or 2D TCPS relative to the tumour xenografts after analyzing the pathways  
27  
28 regulating cell survival and cell fate between the *in vitro* models and tumour xenografts of MDA-  
29  
30 MB-231-H2N cells (Fig. 4f).  
31  
32  
33  
34

35  
36 When triple-negative breast cancer (TNBC) MDA-MB-468 cells were cultured in HA-  
37  
38 oxime gels, Matrigel or 2D TCPS, a similar number of genes were downregulated compared to the  
39  
40 xenograft tumours (125, 134 and 122, respectively) while the number of upregulated genes was  
41  
42 higher in 2D TCPS (94) versus HA-oxime and Matrigel (60 and 54 genes, respectively) (Fig. 4g,  
43  
44 h, Table S4). Subsequent analysis of affected pathways revealed that the hedgehog pathway was  
45  
46 altered when cultured in HA-oxime, Matrigel or 2D TCPS relative to the tumour xenografts (Fig.  
47  
48 4i). Since only 30% of triple-negative breast cancers involve paracrine hedgehog (Hh) signalling,  
49  
50 which has been studied in the context of cancer-associated fibroblasts, co-culture models may be  
51  
52 required to target this pathway.<sup>[40]</sup>  
53  
54  
55  
56  
57  
58  
59  
60  
61  
62  
63  
64  
65

1  
2  
3  
4 Our gene expression pathway analyses show that the JAK-STAT pathway was altered in  
5  
6 both HER2<sup>+</sup> BT474 and MDA-MB-231-H2N cell lines when cultured in Matrigel or on 2D TCPS  
7  
8 relative to xenograft and HA-oxime. This underlines the need to evaluate drugs targeting specific  
9  
10 pathways on validated models. Remarkably, while Matrigel is thought to be the gold standard for  
11  
12 in vitro culture, it has not been benchmarked previously and our data clearly demonstrate that it is  
13  
14 sub-optimal. Overall, HA-oxime gels were the most similar to xenografts, with only 294  
15  
16 differentially expressed genes vs. 434 for Matrigel and 371 for 2D TCPS (Figure 4j, Fig. S14).  
17  
18 The number of differentially expressed genes for the same cell lines was similar between HA-  
19  
20 oxime and HA-oxime-Ln hydrogels (294 versus 308 genes, respectively) compared to the  
21  
22 xenograft tumours (Fig. S14b). Thus, 3D culture reduces, but does not eliminate, differences in  
23  
24 gene expression between 2D culture and xenografts. 3D culture in HA-oxime better emulates the  
25  
26 gene expression profile of xenografts than culture in Matrigel.  
27  
28  
29  
30  
31  
32  
33  
34  
35  
36  
37  
38  
39  
40  
41  
42  
43  
44  
45  
46  
47  
48  
49  
50  
51  
52  
53  
54  
55  
56  
57  
58  
59  
60  
61  
62  
63  
64  
65

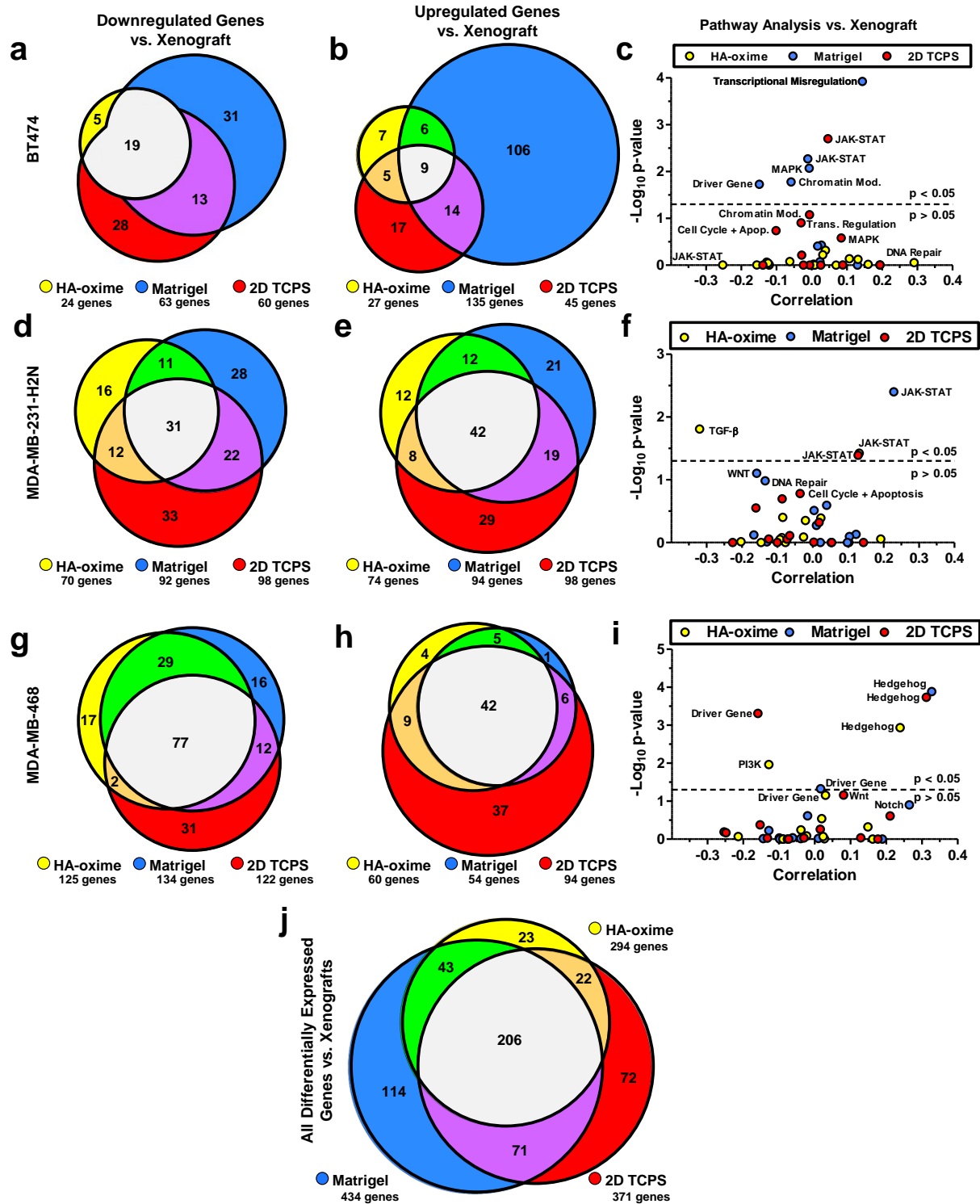


**Figure 4.** Comparison of *in vitro* gene expression and pathway analysis for three breast cancer cell lines relative to tumour xenografts in mice. (a, b) Venn Diagrams depicting the number genes

1  
2  
3  
4 differentially expressed by BT474 cells cultured *in vitro* compared to xenografts. (c) Pathway  
5  
6 specific expression correlation values and p-values by gene set variation analysis of BT474 cells  
7  
8 cultured *in vitro* versus tumour xenografts. Altered pathways in cells cultured *in vitro* are shown  
9  
10 above the dashed line. (d, e) Venn diagrams depicting the number genes differentially expressed  
11  
12 by MDA-MB-231-H2N cells cultured *in vitro* compared to xenografts. (f) Pathway specific  
13  
14 expression correlation values and p-values by gene set variation analysis of MDA-MB-231-H2N  
15  
16 cells cultured *in vitro* versus tumour xenografts. Altered pathways in cells cultured *in vitro* are  
17  
18 shown above the dashed line. (g, h) Venn Diagrams depicting the number genes differentially  
19  
20 expressed by MDA-MB-468 cells cultured *in vitro* compared to xenografts. (i) Pathway specific  
21  
22 expression correlation values and p-values by gene set variation analysis of MDA-MB-468 cells  
23  
24 cultured *in vitro* versus tumour xenografts. Altered pathways in cells cultured *in vitro* are shown  
25  
26 above the dashed line. Pathway specific expression correlation values and p-values by gene set  
27  
28 variation analysis versus tumour xenografts. (j) Summary of all observed differentially expressed  
29  
30 genes after culture in HA-oxime, Matrigel, or 2D TCPS versus mouse xenograft tumours for  
31  
32 BT474, MDA-MB-231-H2N, and MDA-MB-468 cells (n = 3 except for BT474 cells grown in  
33  
34 Matrigel where n = 4).

### 44 **Evaluating Differences in Drug Response Between 2D and 3D Models**

45  
46 To understand if these differences in gene expression could influence cell response in drug  
47  
48 screening, we specifically chose drugs that target pathways differentially expressed between  
49  
50 xenograft and *in vitro* culture in Matrigel and 2D TCPS and that were not differentially expressed  
51  
52 in HA-oxime (Table S4, S5). We tested a series of drugs that target the MAPK (such as Rac  
53  
54 signaling) and JAK-STAT pathways of BT474 cells grown in HA-oxime vs. Matrigel and 2D  
55  
56 TCPS.  
57  
58  
59  
60  
61  
62  
63  
64  
65



BT474 cells treated with EHT-1864 (Rac inhibitor, targeting the MAPK/ERK pathway) were more responsive when cultured in HA-oxime than in Matrigel (Fig. 5a, Fig. S15). In addition, BT474 cells cultured in HA-oxime were more responsive to AZD6482 (PI3K $\beta$  inhibitor involved in the JAK-STAT pathway) than those cultured in Matrigel or on 2D TCPS (Fig. 5b). To gain biological insight into the mechanism underlying the observed differences in drug responsiveness, we quantified the number of genes involved in MAPK and JAK-STAT signaling pathways with differential expression levels relative to tumour xenografts: cells cultured in HA-oxime had fewer differentially expressed genes (14 for MAPK and 4 for JAK-STAT) compared to cells cultured in both Matrigel (43 for MAPK and 29 for JAK-STAT) and on 2D TCPS (23 for MAPK and 10 for JAK-STAT) (Fig. 5c-e, red circles for MAPK and green circles for JAK-STAT). Together these results demonstrate the superiority of HA-oxime over Matrigel and 2D TCPS in drug screening where specific pathways are targeted.

Interestingly, cells cultured in HA-oxime were over tenfold more sensitive to maritoclax (Fig. S15c), an Mcl-1 inhibitor which prevents the normal anti-apoptotic signaling by Mcl-1 on the mitochondria resulting in apoptosis, with an IC<sub>50</sub> of 0.59  $\mu$ M than those cultured in 2D TCPS with IC<sub>50</sub> of 5.5  $\mu$ M (Fig. 5f). Moreover, primary, human patient tumour luminal B breast cancer cells were significantly more sensitive to maritoclax when cultured in 3D HA-oxime than those cultured on 2D TCPS as well, demonstrating both the potential of the HA-oxime hydrogels in personalized medicine and the importance of culture conditions in drug screening (Fig. S16). Maritoclax targets the apoptosis pathway as an inhibitor of anti-apoptotic protein Mcl-1 on the mitochondria. Regulators of this apoptosis pathway, BAD (pro-apoptotic) and BCL2 (anti-apoptotic), had decreased levels in BT474 cells cultured on 2D TCPS relative to 3D culture, which explains the observed differences in drug response (Fig. 5g).

1  
2  
3  
4 We highlight the results of the *in vitro* drug screening performed with BT474 cells where  
5  
6  
7 IC<sub>50</sub> values differed between HA-oxime, Matrigel and 2D TCPS (Fig. 5h). Since the decision to  
8  
9 test drugs in animal models of disease is often based on *in vitro* screening, maritoclax, EHT-1864  
10  
11 and AZD6482 would have been excluded based on culture in Matrigel and/or 2D TCPS, thereby  
12  
13 reflecting the importance of culture in a representative matrix, such as HA-oxime. The differences  
14  
15 between 2D and 3D culture of breast cancer cells are significant in terms of gene expression and  
16  
17 drug response. While cell response did not always differ between the 3 culture conditions (as  
18  
19 shown with ZSTK474 and afatinib, Fig. S15), to ensure comprehensive screening, a validated,  
20  
21 representative system, like HA-oxime, is required.  
22  
23  
24  
25  
26  
27  
28  
29  
30  
31  
32  
33  
34  
35  
36  
37  
38  
39  
40  
41  
42  
43  
44  
45  
46  
47  
48  
49  
50  
51  
52  
53  
54  
55  
56  
57  
58  
59  
60  
61  
62  
63  
64  
65

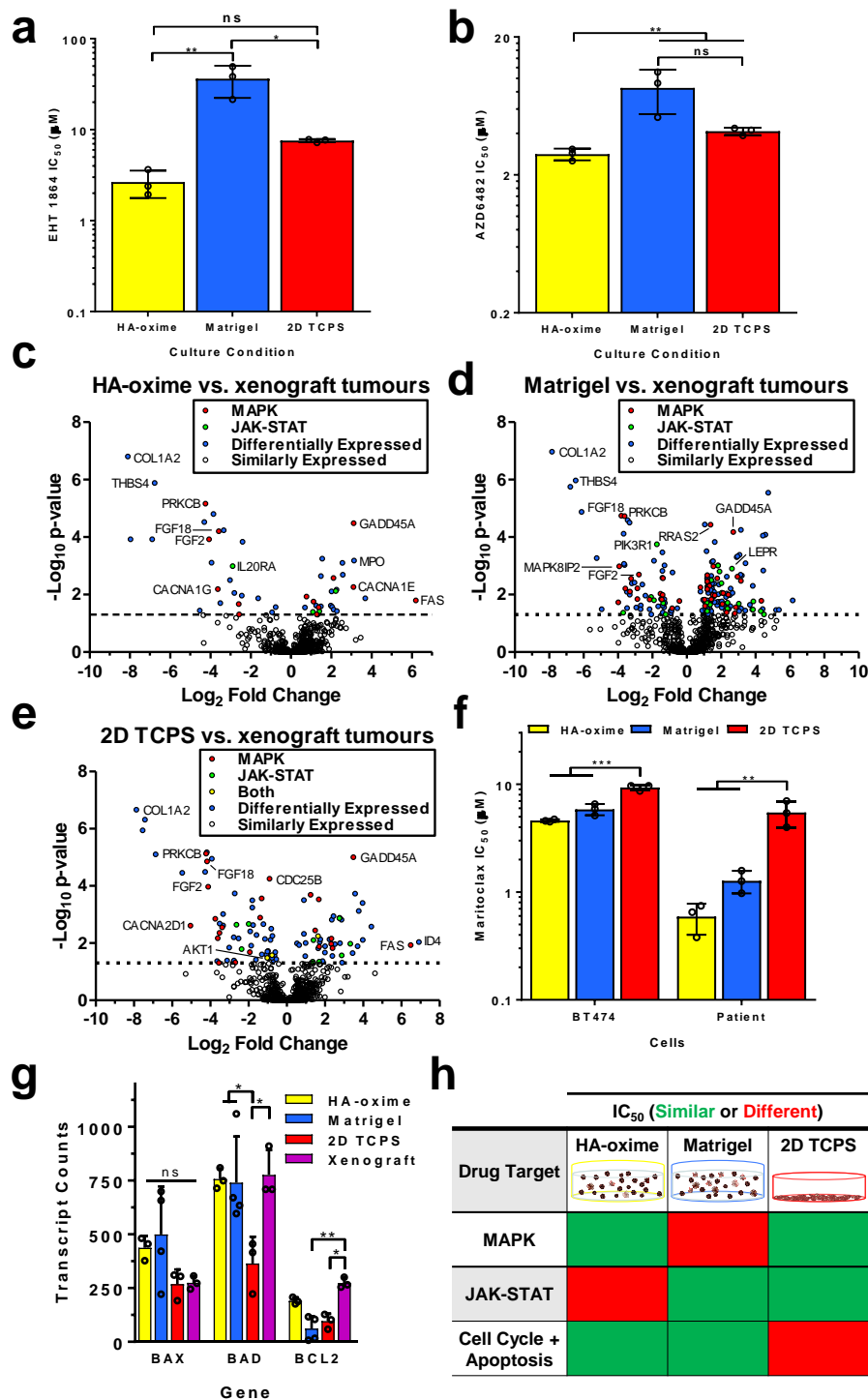


**Figure 5.** Targeting pathways in BT474 breast cancer cells cultured *in vitro* with drugs. (a, b)  $IC_{50}$  values for BT474 cells cultured *in vitro* treated with (a) EHT 1864 targeting the MAPK pathway or (b) AZD6482 targeting the JAK-STAT pathway (n = 3 independent experiments; mean +

standard deviation plotted, \* $p < 0.05$ , \*\* $p < 0.01$ , by one-way ANOVA, Tukey's post-hoc test). (c-d) Volcano plots of differentially expressed genes involved in MAPK signalling (red), JAK-STAT signalling (green), both pathways (yellow), other (blue) and similarly expressed (white) when cultured in (c) HA-oxime, (d) Matrigel or on (e) 2D TCPS versus tumour xenografts. (f)  $IC_{50}$  values for BT474 and patient derived breast cancer cells cultured *in vitro* treated with maritoclax targeting the apoptosis pathway ( $n = 3$  independent experiments; mean + standard deviation plotted, \*\* $p < 0.01$ , \*\*\* $p < 0.001$  by one-way ANOVA, Tukey's post-hoc test). (g) Gene expression counts of apoptosis signalling genes BAX, BAD and BCL2 for BT474 cells cultured *in vitro* or as tumour xenografts. (h) Summary of observed statistical differences in  $IC_{50}$  values from drug screening with EHT 1864 (which targets MAPK), AZD6482 (which targets JAK-STAT) and maritoclax (which targets apoptosis) with BT474 cells cultured in HA-oxime, Matrigel or on 2D TCPS.  $IC_{50}$  values that were statistically different depending on culture platform are shown in red while those which were not statistically different are shown in green.

To gain insight into the broader utility of the HA-oxime hydrogels with other cell types, we investigated the efficacy of erlotinib, an EGFR inhibitor, against TNBC MDA-MB-468 cells. Cells that were grown on 2D TCPS, in Matrigel or HA-oxime for 21 days and treated with erlotinib for 7 days had a significantly higher  $IC_{50}$  of 37.6  $\mu M$  ( $p < 0.01$ ) compared to those cultured in 3D of  $\sim 4.5 \mu M$  (Fig. S17). MDA-MB-468 cells cultured on 2D were less sensitive to erlotinib than other cancer cell lines, despite its established effectiveness in breast cancer xenografts in mice,<sup>[41]</sup> further highlighting the importance of relevant screening assays.

## Conclusions

3D cell culture has several features which make it attractive for drug screening, yet is limited by the use of Matrigel, which does not faithfully recapitulate the gene expression profile of the tumour

1  
2  
3  
4 xenograft and is chemically ill-defined. The newly synthesized HA-oxime hydrogels have  
5  
6 controlled and tunable gelation, mechanical properties, and chemical properties that mimic the  
7  
8 breast ECM, which are not possible with 2D TCPS and limited with Matrigel. By benchmarking  
9  
10 to the *in vivo* gold standard for the first time, we demonstrate that breast cancer cells grown in HA-  
11  
12 oxime hydrogels most closely resemble orthotopic xenografts in terms of gene expression profiles  
13  
14 of 3 distinct breast cancer subtypes. This impacts the value of in vitro drug screening. Formulating  
15  
16 the HA-oxime hydrogels with laminin did not reduce the number of differentially expressed genes  
17  
18 expressed by the breast cancer spheroids compared to the tumour xenografts. Our analysis of  
19  
20 canonical signaling pathways using the gene expression data suggest breast cancer subtype-  
21  
22 dependant changes to gene expression with culture platform. We demonstrated the ability to grow  
23  
24 patient-derived breast cancer cells in HA-oxime hydrogels and thereby identify relevant drug  
25  
26 candidates. Thus, hyaluronan-oxime hydrogels bridge the gap between 2D drug screening *in vitro*  
27  
28 and *in vivo* mouse xenograft models, opening the door to personalized medicine and more  
29  
30 predictive drug screening. To take full advantage of this opportunity, scale up and simultaneous  
31  
32 screening of multiple drugs is required. This well-defined hydrogel platform opens up the  
33  
34 possibility for more complex 3D models with co-culture of multiple cell types, thereby better  
35  
36 emulating the complexity of tumours.  
37  
38  
39  
40  
41  
42  
43  
44

## 45 46 **Acknowledgements**

47  
48 We are grateful for funding from the Natural Sciences and Engineering Research Council of  
49  
50 Canada (Discovery grant to MSS, and CGSD to AEGB and LCB, PGSD to ANG) and the  
51  
52 Canadian Institute for Health Research (Foundation grant to MSS). We acknowledge the Canadian  
53  
54 Foundation for Innovation, project number 19119, and the Ontario Research Fund for funding of  
55  
56 the Centre for Spectroscopic Investigation of Complex Organic Molecules and Polymers. We  
57  
58  
59  
60  
61  
62  
63  
64  
65

thank Dr. Robert Kerbel (Sunnybrook Health Science Centre) for generously providing us with the MDA-MB-231-H2N cell line. We thank members of the Shoichet Lab for thoughtful review of this paper. We thank Laura Smith for the synthesis of monofunctional HA-methylfuran, and Sarah Chagri, Tobias Bauer and Erik Kersten for their contributions.

## Methods

Detailed methods are presented in the Supplementary Information.

## References

- [1] S. P. Leelananda, S. Lindert, Beilstein J Org Chem 2016, 12, 2694; V. Malik, J. K. Dhanjal, A. Kumari, N. Radhakrishnan, K. Singh, D. Sundar, Methods 2017, 131, 10.
- [2] Y. Li, E. Kumacheva, Sci Adv 2018, 4.
- [3] N. Jacobi, R. Seeboeck, E. Hofmann, H. Schweiger, V. Smolinska, T. Mohr, A. Boyer, W. Sommergruber, P. Lechner, C. Pichler-Huebschmann, K. Onder, H. Hundsberger, C. Wiesner, A. Eger, Oncotarget 2017, 8, 107423.
- [4] T. Hasan, B. Carter, N. Denic, L. Gai, J. Power, K. Voisey, K. R. Kao, J Clin Pathol 2015, 68, 746.
- [5] C.-P. Day, G. Merlino, T. Van Dyke, Cell 2015, 163, 39.
- [6] A. Ivascu, M. Kubbies, International journal of oncology 2007, 31, 1403; J. R. Todd, K. A. Ryall, S. Vyse, J. P. Wong, R. C. Natrajan, Y. Yuan, A. C. Tan, P. H. Huang, Oncotarget 2016, 7, 62939; Y. Imamura, T. Mukohara, Y. Shimono, Y. Funakoshi, N. Chayahara, M. Toyoda, N. Kiyota, S. Takao, S. Kono, T. Nakatsura, H. Minami, Oncology reports 2015, 33, 1837.
- [7] F. Madoux, A. Tanner, M. Vessels, L. Willetts, S. Hou, L. Scampavia, T. P. Spicer, SLAS Discov 2017, 22, 516.
- [8] E. R. Boghaert, X. Lu, P. E. Hessler, T. P. McGonigal, A. Oleksijew, M. J. Mitten, K. Foster-Duke, J. A. Hickson, V. E. Santo, C. Brito, T. Uziel, K. S. Vaidya, Neoplasia 2017, 19, 695.
- [9] J. E. Sero, H. Z. Sailem, R. C. Ardy, H. Almuttaqi, T. Zhang, C. Bakal, Mol Syst Biol 2015, 11, 0790; M. F. Gencoglu, L. E. Barney, C. L. Hall, E. A. Brooks, A. D. Schwartz, D. C. Corbett, K. R. Stevens, S. R. Peyton, ACS Biomater Sci Eng 2018, 4, 410.
- [10] R. Xu, J.-H. Mao, Integr Biol 2011, 3, 368; C. J. Lovitt, T. B. Shelper, V. M. Avery, BMC Cancer 2018, 18, 41.
- [11] B. Weigelt, C. M. Ghajar, M. J. Bissell, Adv Drug Deliv Rev 2014, 69-70, 42.
- [12] C. S. Hughes, L. M. Postovit, G. A. Lajoie, Proteomics 2010, 10, 1886.
- [13] L. Lambricht, P. De Berdt, J. Vanacker, J. Leprince, A. Diogenes, H. Goldansaz, C. Bouzin, V. Pr  at, C. Dupont-Gillain, A. d. Rieux, Dent Mater 2014, 30, e349.
- [14] P. Auvinen, R. Tammi, J. Parkkinen, M. Tammi, U. Agren, R. Johansson, P. Hirvikoski, M. Eskelinen, V. M. Kosma, Am J Pathol 2000, 156, 529.
- [15] A. Rizwan, M. Cheng, Z. M. Bhujwalla, B. Krishnamachary, L. Jiang, K. Glunde, NPJ Breast Cancer 2015, 1, 15017; J. R. Todd, K. A. Ryall, S. Vyse, J. P. Wong, R. C. Natrajan, Y. Yuan, A.-C. Tan, P. H. Huang, Oncotarget 2016, 7, 62939.

- [16] H. Wang, D. Zhu, A. Paul, L. Cai, A. Enejder, F. Yang, S. C. Heilshorn, *Advanced Functional Materials* 2017, 27, 1605609.
- [17] F. Saito, H. Noda, J. W. Bode, *ACS chemical biology* 2015, 10, 1026.
- [18] S. A. Fisher, A. E. G. Baker, M. S. Shoichet, *J Am Chem Soc* 2017, 139, 7416.
- [19] A. K. Jha, K. M. Tharp, S. Browne, J. Ye, A. Stahl, Y. Yeghiazarians, K. E. Healy, *Biomaterials* 2016, 89, 136.
- [20] J. Kalia, R. T. Raines, *Angew Chem Int Ed* 2008, 47, 7523; C. Kascholke, T. Loth, C. Kohn-Polster, S. Möller, P. Bellstedt, M. Schulz-Siegmund, M. Schnabelrauch, M. C. Hacker, *Biomacromolecules* 2017, 18, 683.
- [21] A. E. G. Baker, R. Y. Tam, M. S. Shoichet, *Biomacromolecules* 2017, 18, 4373.
- [22] H.-H. Lin, H.-K. Lin, I. H. Lin, Y.-W. Chiou, H.-W. Chen, C.-Y. Liu, H. I. C. Harn, W.-T. Chiu, Y.-K. Wang, M.-R. Shen, M.-J. Tang, *Oncotarget* 2015, 6, 20946.
- [23] M. Smolina, E. Goormaghtigh, *Analyst* 2016, 141, 620.
- [24] M. J. Paszek, N. Zahir, K. R. Johnson, J. N. Lakins, G. I. Rozenberg, A. Gefen, C. A. Reinhart-King, S. S. Margulies, M. Dembo, D. Boettiger, D. A. Hammer, V. M. Weaver, *Cancer cell* 2005, 8, 241.
- [25] K. R. Levental, H. Yu, L. Kass, J. N. Lakins, M. Egeblad, J. T. Erler, S. F. T. Fong, K. Csiszar, A. Giaccia, W. Weninger, M. Yamauchi, D. L. Gasser, V. M. Weaver, *Cell* 2009, 139, 891; A. Ansardamavandi, M. Tafazzoli-Shadpour, R. Omidvar, I. Jahanzad, *J Mech Behav Biomed Mater* 2016, 60, 234.
- [26] L. Edjekouane, S. Benhadjeba, M. Jangal, H. Fleury, N. Gévry, E. Carmona, A. Tremblay, *Oncotarget* 2016, 7, 77276; H. Tan, H. Li, J. P. Rubin, K. G. Marra, *Journal of tissue engineering and regenerative medicine* 2011, 5, 790.
- [27] A. S. Caldwell, G. T. Campbell, K. M. T. Shekiri, K. S. Anseth, *Adv Healthc Mater* 2017, 6, 1700254; S. Suri, C. E. Schmidt, *Tissue engineering. Part A* 2010, 16, 1703; Z.-N. Zhang, B. C. Freitas, H. Qian, J. Lux, A. Acab, C. A. Trujillo, R. H. Herai, V. A. Nguyen Huu, J. H. Wen, S. Joshi-Barr, J. V. Karpiak, A. J. Engler, X.-D. Fu, A. R. Muotri, A. Almutairi, *Proc Natl Acad Sci* 2016, 113, 3185.
- [28] M. Rinaudo, *Int J Biol Macromol* 2008, 43, 444.
- [29] S. E. Stabenfeldt, A. J. Garcia, M. C. LaPlaca, *Journal of biomedical materials research. Part A* 2006, 77, 718.
- [30] S. Godar, T. A. Ince, G. W. Bell, D. Feldser, J. L. Donaher, J. Bergh, A. Liu, K. Miu, R. S. Watnick, F. Reinhardt, S. S. McAllister, T. Jacks, R. A. Weinberg, *Cell* 2008, 134, 62; K. To, A. Fotovati, K. M. Reipas, J. H. Law, K. Hu, J. Wang, A. Astanehe, A. H. Davies, L. Lee, A. L. Stratford, A. Raouf, P. Johnson, I. M. Berquin, H. D. Royer, C. J. Eaves, S. E. Dunn, *Cancer Res* 2010, 70, 2840; R. Castello-Cros, D. R. Khan, J. Simons, M. Valianou, E. Cukierman, *BMC Cancer* 2009, 9, 94.
- [31] G. Wang, T. Zhao, X. Song, W. Zhong, L. Yu, W. Hua, M. M. Q. Xing, X. Qiu, *Polymer Chemistry* 2015, 6, 283; S. Riffle, R. N. Pandey, M. Albert, R. S. Hegde, *BMC Cancer* 2017, 17, 338.
- [32] P. Heldin, K. Basu, B. Olofsson, H. Porsch, I. Kozlova, K. Kahata, *J Biochem* 2013, 154, 395; P. Auvinen, R. Tammi, V.-M. Kosma, R. Sironen, Y. Soini, A. Mannermaa, R. Tumelius, E. Uljas, M. Tammi, *Int. J. Cancer* 2013, 132, 531.
- [33] E. Curcio, S. Salerno, G. Barbieri, L. De Bartolo, E. Drioli, A. Bader, *Biomaterials* 2007, 28, 5487.

- [34] S. Ingthorsson, K. Andersen, B. Hilmarsdottir, G. M. Maelandsmo, M. K. Magnusson, T. Gudjonsson, *Oncogene* 2015, 35, 4244.
- [35] M. A. Aleskandarany, E. A. Rakha, M. A. Ahmed, D. G. Powe, E. C. Paish, R. D. Macmillan, I. O. Ellis, A. R. Green, *Breast Cancer Res Treat* 2010, 122, 45.
- [36] J. A. Menendez, R. Lupu, *Expert opinion on therapeutic targets* 2017, 21, 1001; M. E. Monaco, *Oncotarget* 2017, 8, 29487.
- [37] N. Mori, F. Wildes, T. Takagi, K. Glunde, Z. M. Bhujwala, *Front Oncol* 2016, 6, 262.
- [38] A. N. Lane, J. Tan, Y. Wang, J. Yan, R. M. Higashi, T. W. M. Fan, *Metab Eng* 2017, 43, 125.
- [39] M. García-Aranda, M. Redondo, *International journal of molecular sciences* 2017, 18, 2543.
- [40] M. N. Hui, A. Cazet, B. Elsworth, D. Roden, T. Cox, J. Yang, A. McFarland, N. Deng, C.-L. Chan, S. O'Toole, A. Swarbrick, *Journal of Clinical Oncology* 2018, 36, e24216.
- [41] F. Yamasaki, D. Zhang, C. Bartholomeusz, T. Sudo, G. N. Hortobagyi, K. Kurisu, N. T. Ueno, *Mol Cancer Ther* 2007, 6, 2168; Y.-K. I. Lau, X. Du, V. Reyannavar, B. Hopkins, J. Shaw, E. Bessler, T. Thomas, M. M. Pires, M. Keniry, R. E. Parsons, S. Cremers, M. Szabolcs, M. A. Maurer, *Oncotarget* 2014, 5, 10503.





[Click here to access/download](#)

**Production Data**

[adma.201901166 Manuscript Highlighted.docx](#)



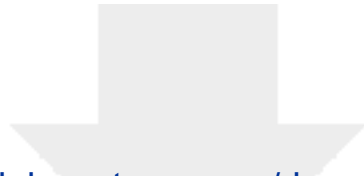


Click here to access/download

**Production Data**

TOC Benchmarking.tif

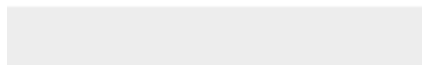
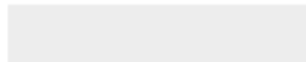


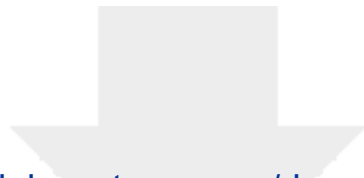


[Click here to access/download](#)

**Production Data**

[adma.201901166 Supplementary.docx](#)





[Click here to access/download](#)

**Production Data**

[adma.201901166 Summary.docx](#)

